Three- and five-nucleon transfers in ^{9}Be$(p,\alpha)^6$Li reaction at 25 and 30 MeV

F. Pellegrini, G. F. Segato, A. Barbadoro, L. Corradi, M. Morando, and P. Pavan
Dipartimento di Fisica, Università di Padova, Istituto Nazionale di Fisica Nucleare, via Marzolo 8, I-35131, Padova, Italy

I. Gabrielli
Dipartimento di Fisica, Università di Trieste, Istituto Nazionale di Fisica Nucleare, via Valerio 2, I-34127, Trieste, Italy
(Received 3 February 1992)

Angular distributions of the ^{9}Be$(p,\alpha)^6$Li reaction leading to the ground and first two excited states of ^{6}Li were measured at incident energies of 25.0 and 30.0 MeV. Both the one-step three- and five-nucleon transfers were considered in the theoretical analysis using current shell-model wave functions. We reproduce fairly well with distorted-wave Born approximation theory the experimental energy dependence of the integrated cross sections for the ground and first excited states of ^{6}Li. A marked disagreement is observed for the second excited state, whose experimental integrated cross section shows a steeper energy dependence than the calculated one.

PACS number(s): 25.40.Hs, 27.20.+n

I. INTRODUCTION

Our previous (p,α) studies on $1p$, $2s$-$1d$ shell nuclei [1,2] have shown that the primary reaction mechanism in the dynamics of these reactions is the three-nucleon pickup which strongly dominates over the knock-out process. On the other hand, in the analysis of (p,α) reactions on target nuclei with mass number $A<10$, it may become important to consider in addition to the light particle pickup (LPPU) the heavy particle pickup (HPPU) process. A recent experimental study of the (p,α) reaction on light nuclei reported in the literature is the ^{9}Be$(p,\alpha)^6$Li reaction investigated between 18 and 45 MeV bombarding energies [3]. The authors of Ref. [3] observed angular distributions which are characterized by a strong rise in forward and backward directions, suggesting that the HPPU may give an important contribution in describing the dynamics of the (p,α) reaction. However, due to the complexity of microscopic calculations involved in the distorted-wave Born approximation (DWBA) theory to compute the coherent contribution of the LPPU and HPPU amplitudes, the authors of Ref. [3] limited their study only to spectroscopic information assuming that the integrated cross sections in the forward and backward directions are a good measure for the relative spectroscopic strengths.

In order to further investigate the (p,α) reaction mechanism and to complete the study on $1p$-shell nuclei we performed the present ^{9}Be$(p,\alpha)^6$Li experiment at incident energies of 25.0 and 30.0 MeV. The aim of this study is twofold, first to see the importance of HPPU in such reactions and second to reproduce with full DWBA calculations the energy dependence of the integrated cross sections not only at our bombarding energies but also in the energy interval between 18 and 45 MeV.

II. EXPERIMENTAL PROCEDURE

The momentum analyzed beam from the XTU Tandem of the National Laboratory of Legnaro provided the source of the proton beam. Self-supporting beryllium foils with a purity of 99.8% and areal density of 185 μg/cm^2 were used as targets. The scattered particles were detected by two ΔE-E telescopes with silicon surface barrier detectors, mounted on a rotatable platform of the scattering chamber. The two telescopes, cooled to -1 °C and angularly separated by 5°, were used to obtain the ^{6}Li and α spectra from 5° to 90° (laboratory) in 5° steps. The thickness of the ΔE detector was 18 μm for the (^{6}Li) heavy particle counter and 38 μm for the α counter. Both E detectors had a thickness of 400 μm. The ΔE and E signals were stored on magnetic tape and then sorted off line, into $\Delta E \times E$ plots, to separate the different ^{6}Li and α particle groups [4]. The ^{6}Li data were primarily used to obtain the (p,α) differential cross sections at backward angles. The elastic proton scattering was measured from $\theta_{\text{c.m.}}=7°$ up to 140° by using a 5-mm lithium-drifted silicon detector.

Absolute cross sections were determined by reference to the elastic ^{9}Be$(p,p)^9$Be optical model calculation and were checked by known target thickness, integrated beam currents and measured solid angles of the detector telescopes. The accuracy of the absolute cross sections thus determined is estimated to be about $\pm 18\%$.

III. EXPERIMENTAL RESULTS AND DISCUSSION

A. Angular distributions and DWBA calculations

Two typical pulse height spectra are shown in Fig. 1, the peaks are labeled by their excitation energy. The energy resolution (full width at half maximum) for the ground-state transitions is 100 and 170 keV for the α and ^{6}Li spectra, respectively. In the ^{6}Li spectrum we could not observe the 2.19 MeV $J^\pi=3^+$, $T=0$ level because it is particle unstable, while the 3.56 MeV $J^\pi=0^+$, $T=1$ state is particle stable, because its energetically allowed breakup in the $\alpha+d$ channel is forbidden by spin, isospin, and parity selection rules.

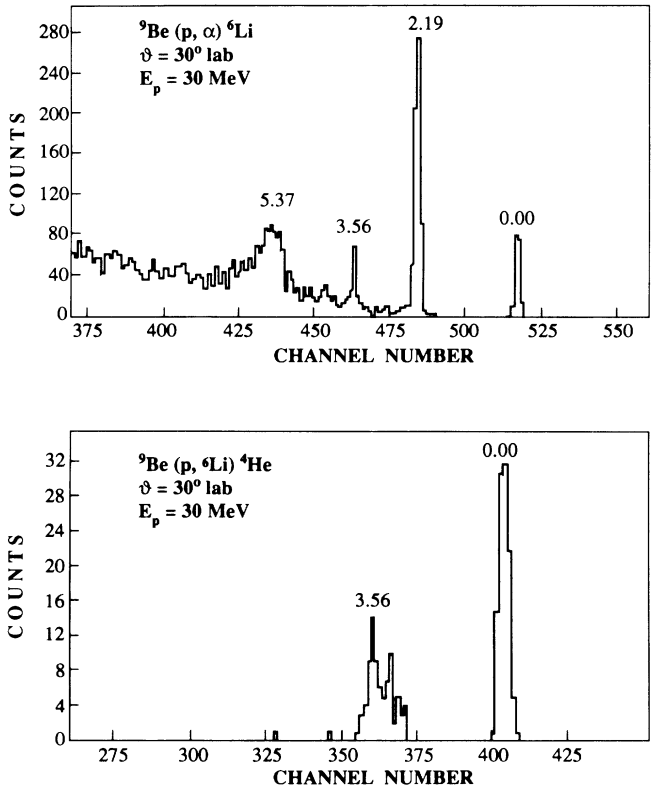

FIG. 1. Alpha and lithium spectra produced on a ^{9}Be target at a proton bombarding energy of 30.0 MeV and $\theta_{lab}=30°$. The peaks are labeled by the ^{6}Li excitation energy expressed in MeV.

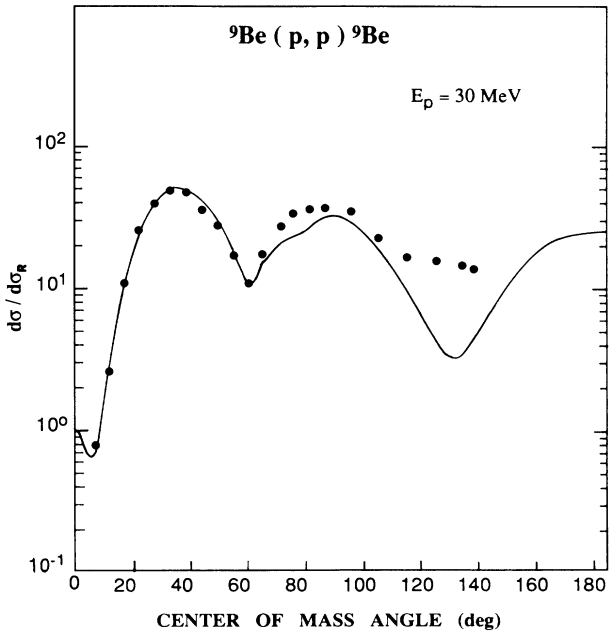

FIG. 2. Experimental points and optical model curve of the 30 MeV proton elastic scattering. The optical potentials are listed in Table I.

In Fig. 2 is reported the experimental elastic differential cross section together with the optical model curve obtained with the potential parameters described in Table I. These parameters were taken from the analysis of elastic scattering of 49.75 MeV protons by ^{9}Be, done by Mani and co-workers [5].

For the analysis of the (p,α) reaction, as mentioned in the introduction, we will consider both the pickup of a light (^{3}H) and heavy (^{5}He) cluster. Including these two transfers we can represent the (p,α) differential cross section for a transition to a state of the residual nucleus with total angular momentum J_f in the following way:

$$\left[\frac{d\sigma}{d\Omega}\right]_{J_f}=\frac{N}{2s_p+1}\sum_{j,m,m_p}\frac{1}{2j+1}\left|\sum_{l,s}\left[\delta_{s,1/2}\sqrt{C^2S(p,{}^3\mathrm{H})}\sqrt{C_T^2S({}^3\mathrm{H},{}^6\mathrm{Li},lj)}f_{l,s,j}^{m,m_p}(\theta)\right.\right.$$
$$+\delta_{j,3/2}r\sqrt{2J_f+1}\left(\sum_{J=0,2}\sqrt{C'^2S({}^5\mathrm{He},{}^4\mathrm{He};J)}\sum_{j'=1/2,3/2}\sqrt{C_T'^2S(p,{}^5\mathrm{He};j')}\right)$$
$$\left.\left.\times f_{l,s,j}^{m,m_p}(\pi-\theta)\right]\right|^2, \quad (1)$$

where N is a normalization factor, s_p and m_p are the proton quantum numbers, j and l are the total and orbital angular momenta of the transferred cluster with intrinsic spin s and projection m, $f(\theta)$ and $f(\pi-\theta)$ are the amplitude cross sections for the light and heavy particle transfers and r is the ratio between HPPU and LPPU amplitudes, whose value can be determined by comparing the calculated cross section with the experimental one.

TABLE I. Optical model parameters used in the ^{9}Be$(p,p)^9$Be elastic channel.

V (MeV)	W (MeV)	$V_{s.o.}$ (MeV)	r_0 (fm)	a (fm)	r_w (fm)	a_w (fm)	$r_{s.o.}$ (fm)	$a_{s.o.}$ (fm)	r_c (fm)
−38.3	−4.84	1.12	1.2	0.61	1.79	0.66	4.9	0.56	1.2

TABLE II. Optical model parameters used for the bound states and exit channel in the ^{9}Be$(p,\alpha)^6$Li reaction.

Channel	V (MeV)	W (MeV)	$4W_s$ (MeV)	r_0[a] (fm)	a_0 (fm)	r_w (fm)	a_w (fm)	r_c[b] (fm)
$\alpha+^6$Li	−98.34	−2.17	18.44	0.506	0.66	2.365	0.383	1.2
$t+^6$Li	c			1.115	0.6			1.2
$\alpha+^5$He	c			2.07	0.2			1.2

[a] The parameter r_0 is defined by $R = r_0(A_t^{1/3} + A_p^{1/3})$, where R is the total radius of potential and t and p stand for target and projectile, respectively.
[b] The Coulomb radius is defined as $r_c A_t^{1/3}$.
[c] Adjusted to reproduce the observed binding energies.

The amplitudes for the two processes are multiplied by the spectroscopic strengths $\sqrt{C^2S}$ of the light and heavy cluster in the target and residual nucleus respectively. The first Kronecker symbol ensures that only one value of the intrinsic spin $s = \frac{1}{2}$ is allowed for the light cluster, while the $\delta_{j,3/2}$ limits the total angular momentum of the heavy cluster only to $j = \frac{3}{2}$. Finally, the two processes are added coherently for the different values of the l and s transfer; in cases where different j transfer values are allowed, the cross sections are added incoherently.

The reaction amplitudes $f(\theta)$ are evaluated in zero range DWBA by means of the computer code DWUCK-5 [6] using, as optical model parameters for the $p+^9$Be channel those given in Table I, and for the other channels the parameters listed in Table II. These last optical parameters have been derived from DeVries *et al.* [7], who studied the ^{9}Be$(p,\alpha)^6$Li ground-state transition at $E_p = 45$ MeV. In Figs. 3–5 are reported the angular distributions at 30 and 25 MeV bombarding energies for the ground ($J^\pi = 1^+$, $T = 0$), for the 2.19 MeV ($J^\pi = 3^+$, $T = 0$), and for the 3.56 MeV ($J^\pi = 0^+$, $T = 1$) states, respectively. The continuous lines are the theoretical calculations as given by (1) with a value of $r = 0.2$, while the dashed lines, shown only at 30 MeV, represent the calculated curves based only on light particle pickup ($r = 0$). From these figures we see that the calculations reproduce the experimental angular distributions within the accuracy usually found for (p,α) reactions on light 1p-shell nuclei [1,2]. However, the inclusion of the heavy particle pickup is of considerable importance to explain the experimental differential cross section in the backward direction. It should be mentioned that the authors of Ref. [7] found at forward angles, in zero-range DWBA calcula-

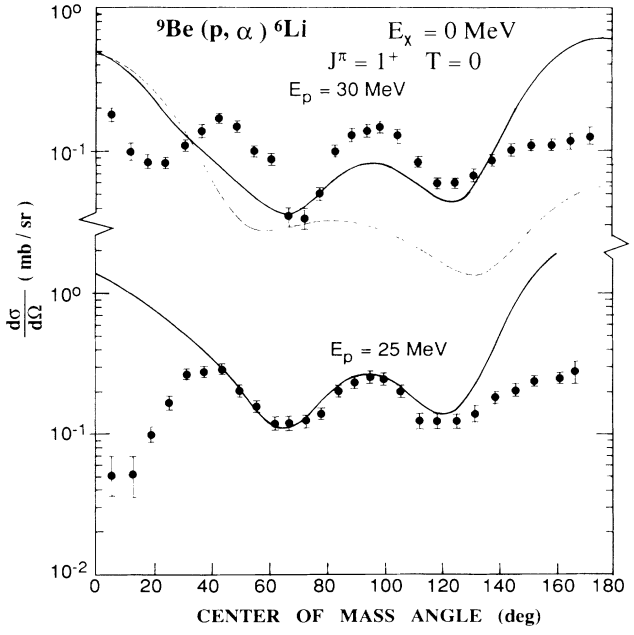

FIG. 3. Experimental and calculated DWBA curves for the ground state transition of the ^{9}Be$(p,\alpha)^6$Li reaction at 30 and 25 MeV. The error bars correspond only to statistical uncertainties, the solid lines represent the coherent and incoherent addition of the LPPU and HPPU amplitudes with an r value equal to 0.2 (see text). The dashed line (shown at 30 MeV) represents the LPPU contribution.

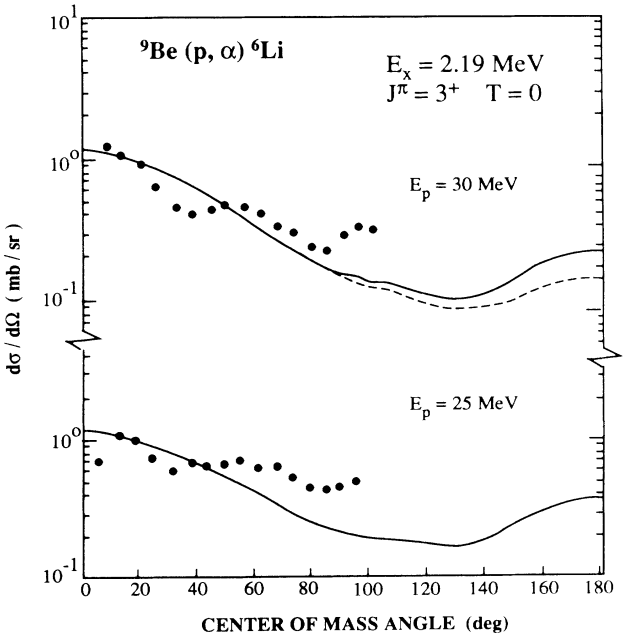

FIG. 4. Experimental and calculated DWBA curves for the 2.19 MeV state transition. The solid and dashed lines are the theoretical curves as explained in the caption of Fig. 3.

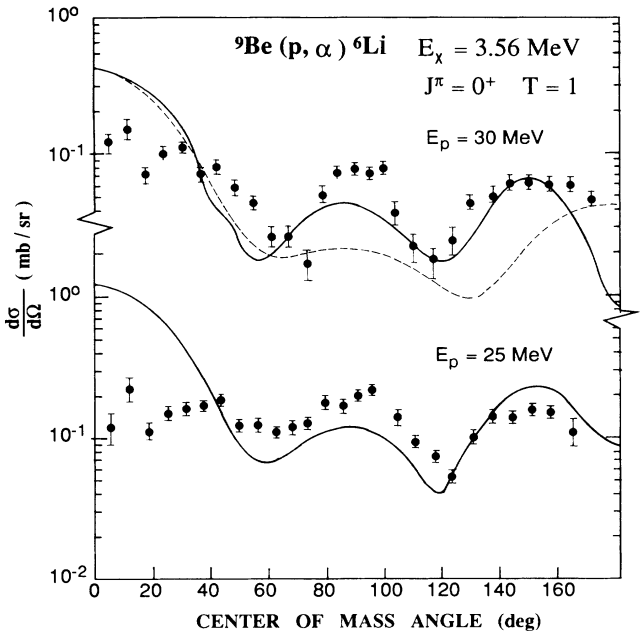

FIG. 5. Experimental and calculated DWBA curves for the 3.56 MeV state. The solid and dashed lines are the theoretical curves as explained in the caption of Fig. 3.

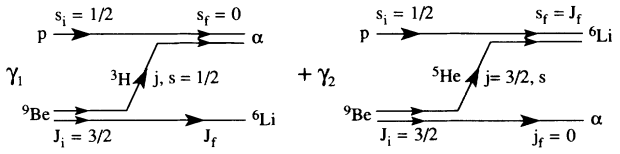

FIG. 6. Diagram illustrating the addition of a light particle pickup (LPPU) and a heavy particle pickup (HPPU) in the ^{9}Be(p,α)^{6}Li reaction. J_i, s_i, J_f, and s_f stand for initial and final angular momentum and spin channels. j and s represent the quantum numbers of the cluster.

tions, a strong HPPU strength compared to the LPPU one. We have not found such an effect using the zero range DWBA by the code DWUCK-5. In all transfers studied we observed a strong LPPU strength at forward angles as it appears clearly in Figs. 3–5 by the dashed lines.

B. Evaluation of spectroscopic amplitudes

Let us consider the diagram shown in Fig. 6, which describes schematically the ^{9}Be(p,α)^{6}Li cross section as given by expression (1).

From analysis of this diagram it is clear that the al-

TABLE III. Spectroscopic strengths for the ^{3}H and ^{5}He transfers in the ^{9}Be(p,α)^{6}Li reaction.

LPPU final state E_x (MeV)	J^π,T	$\sqrt{C^2S(p,^3\mathrm{H})}$[a]	$\sqrt{C_T^2S(^3\mathrm{H},^6\mathrm{Li};lj)}$[a]	Transfer[b] quantum numbers N,l,s,j
0	$1^+,0$	1.41	0.186 $l=1$ $j=\frac{1}{2}$	$1,1,\frac{1}{2},\frac{1}{2}$
			0.150 $l=1$ $j=\frac{3}{2}$	$1,1,\frac{1}{2},\frac{3}{2}$
			−0.029 $l=3$ $j=\frac{5}{2}$	$0,3,\frac{1}{2},\frac{5}{2}$
2.19	$3^+,0$	1.41	0.533 $l=1$ $j=\frac{3}{2}$	$1,1,\frac{1}{2},\frac{3}{2}$
			0.136 $l=3$ $j=\frac{5}{2}$	$0,3,\frac{1}{2},\frac{5}{2}$
			0.548 $l=3$ $j=\frac{7}{2}$	$0,3,\frac{1}{2},\frac{7}{2}$
3.56	$0^+,1$	1.41	0.165 $l=1$ $j=\frac{3}{2}$	$1,1,\frac{1}{2},\frac{3}{2}$
HPPU final state E_x (MeV)	J^π,T	$\sqrt{C'^2S(^5\mathrm{He},^4\mathrm{He};J)}$[a]	$\sqrt{C_T'^2S(p,^5\mathrm{He};j')}$[a]	Transfer[b] quantum numbers l,s,j
0	$1^+,0$	−0.750 $J=0(2S)$	0.564 $j'=\frac{3}{2}$	$1,\frac{1}{2},\frac{3}{2}$
		0.744 $J=2(1D)$	−0.580 $j'=\frac{1}{2}$	$1,\frac{3}{2},\frac{3}{2}$
				$3,\frac{3}{2},\frac{3}{2}$
2.19	$3^+,0$	0.744 $J=2(1D)$	1.000 $j'=\frac{3}{2}$	$1,\frac{5}{2},\frac{3}{2}$
				$3,\frac{5}{2},\frac{3}{2}$
3.56	$0^+,1$	0.744 $J=2(1D)$	−0.830 $j'=\frac{3}{2}$	$1,\frac{1}{2},\frac{3}{2}$

[a] The C^2 are the isospin vector couplings and their values are given by $C^2=0.5$, $C'^2=1$, $C_T^2=1$ for $T=0$ and $\frac{1}{3}$ for $T=1$, $C_T'^2=\frac{1}{2}$ for both $T=0$ and 1.

[b] The reaction amplitudes multiplied by the respective spectroscopic strengths are added coherently for the $j=\frac{3}{2}$ transfer independently of the l and s quantum numbers, otherwise are added incoherently. The quantum numbers N and l are fixed by the conservation of oscillator quanta $2N+l=3$ for LPPU and $2N+L=4$ for HPPU with $L=0$ and 2 ($2S,1D$).

lowed channel spin for the ^{3}H transfer is only $\frac{1}{2}$, because it combines with the proton spin to obtain a zero value of the α-channel spin. In addition it is evident that for the total angular momentum of the ^{5}He transfer only one value for $j=\frac{3}{2}$ is permitted, in order to leave the α partner in the target nucleus with a zero total angular momentum. The relevant spectroscopic amplitudes describing the transfers shown in Fig. 6 are those which involve the projectile in the $p+{}^3\mathrm{H}\rightarrow\alpha$ and $p+{}^5\mathrm{He}\rightarrow{}^6\mathrm{Li}$ channels and the ^{9}Be target nucleus in the ^{6}Li+^{3}H and ^{5}He+α channels, respectively.

The spectroscopic amplitudes of the projectile in the α particle is given simply by $\sqrt{2}$, while the spectroscopic strengths of the proton in the residual nucleus can be obtained by ^{6}Li shell model calculations using for instance the $1p$ effective interaction of Cohen and Kurath [8]. The calculated ^{6}Li level scheme together with the experimental one is shown in Fig. 7. The adopted values of the two-body matrix elements are those reported in Table 6 of Ref. [8] and labeled as (6–16)2BME. Finally for the spectroscopic amplitudes of the target nucleus involved in both processes we have taken those calculated by Kurath and Millener [9] for the ^{3}H cluster and by Kurath [10] for the ^{5}He cluster in ^{9}Be target nucleus. All the spectroscopic strengths thus derived with the proper sign are reported in Table III.

These shell-model calculations are based on the $0\hbar\omega$ model space, in which the s shell is completely filled and only the p shell is active. It is worthwhile to mention that van Hees and Glaudemans [11] improved these shell-model calculations including excitation of particles in the $2s$-$1d$ shell or holes in the $1s$ shell, expanding the $0\hbar\omega$ to the $(0+1)\hbar\omega$ model space. Recently Wolters and coworkers [12] considered a complete $(0+2)\hbar\omega$ model space for the $A=4$–16 p-shell nuclei. It is interesting to remark that the authors of Ref. [12] found for the lowest levels in the nuclear mass region $A\leq 10$ that the $0\hbar\omega$ component account almost for 80%–70% of the structure of their wave functions. Finally Nadasen *et al.* [13] in the study of the ^{9}Be$(p,p\alpha)^5$He cluster knock-out reaction at 200 MeV, derived from the experimental data spectroscopic strengths for the ^{4}He cluster in ^{9}Be, which compare very well with shell-model predictions of the $0\hbar\omega$ model space.

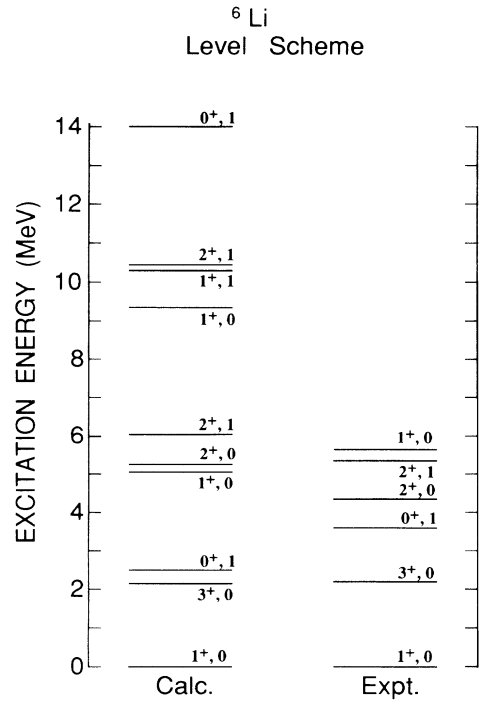

FIG. 7. Comparison of the calculated ^{6}Li spectrum in the $0\hbar\omega$ model space with the experimental one.

C. Energy dependence of the integrated cross sections

Figure 8 shows the energy dependence of the experimental integrated cross sections (10°–170°) for the ground and second excited states, while for the first excited state at 2.19 MeV is reported only the integrated cross section from 10°–90°. The continuous and dashed lines are the corresponding theoretical curves as given by in-

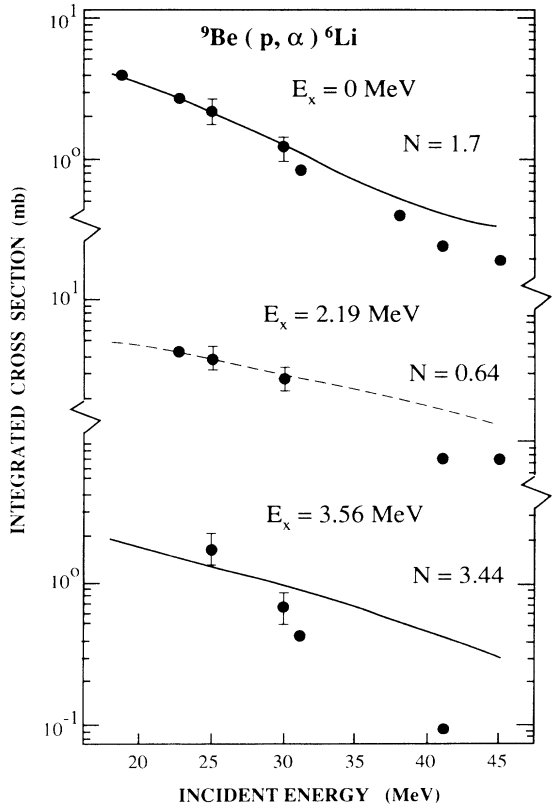

FIG. 8. Energy dependence of the integrated cross sections for the ^{9}Be$(p,\alpha)^6$Li reaction leading to ground, 2.19 and 3.56 MeV states. The experimental points with total error bars are obtained in the present experiment, while the other points are from Ref. [3]. The continuous and dashed lines represent the calculated values obtained by integration of expression (1) (see text) in the angular interval 0°–180° (continuous line) and 0°–90° (dashed line). The N values reported represent the normalization factors of the cross sections.

tegration of expression (1). The optical model parameters reported in Tables I and II have been used for the whole energy interval. The experimental points at 25 and 30 MeV with error bars, which include all uncertainties, are obtained from the present experiment, while those at lower and higher bombarding energies are results reported by Hauser *et al.* [3]. It should be pointed out that our integrated cross sections, taking into account the energy dependence, are about 20% larger than the corresponding ones at 31 MeV obtained in Ref. [3]. In Fig. 8 are shown also the N values of the normalization factors used in reproducing the experimental values of the integrated cross sections. The energy dependence is fairly well reproduced for the ground and 2.19 MeV states, but there is a particular disagreement for the 3.56 MeV state, whose experimental integrated cross section shows a steeper energy dependence than the calculated one. Hauser *et al.* [3] fitted the energy dependence data by an exponential law $\sigma \propto E^{-n}$ with different n values. For instance the n value deduced for the ground state transition is 2.68, while for the 3.56 MeV cross section an exponent $n=3.55$ has been found. Now this anomaly has been confirmed by our DWBA calculations. The failure in reproducing the 3.56 MeV experimental energy dependence is an evident signature that more complex degrees of freedom are involved in the reaction dynamics than the simple one-step transfer processes assumed in our analysis.

IV. CONCLUSIONS

The present study of the ^{9}Be$(p,\alpha)^6$Li reaction at energies of 25 and 30 MeV has shown angular distributions to the ground and to the first two excited states, with prominent forward and backward enhancement of the differential cross section. Although the triton pickup process is the dominant (p,α) reaction mechanism, it is important to consider heavier cluster pickup for light $1p$ shell target nuclei in order to reproduce the backward peak of the experimental angular distributions. Considering a ratio equal to 0.2 between the amplitudes of HPPU and LPPU transfers we have obtained a reasonable agreement with the experimental data. The energy dependence of the integrated cross sections is well reproduced by DWBA calculations for the transitions to the ground and first excited state. Disagreement is observed for the 3.56 MeV state transition, which experimentally shows a much steeper dependence with energy than the calculated one. This behavior is a manifestation that other degrees of freedom are involved, different from the one-step cluster transfer processes assumed in our calculations.

The authors wish to acknowledge the precious assistance during the experiment of A. Dal Bello.

[1] A. Barbadoro, D. Consolaro, F. Pellegrini, G. F. Segato, and I. Gabrielli, Phys. Rev. C **38**, 517 (1988).
[2] F. Pellegrini, D. Trivisonno, S. Avon, R. Bianchin, and R. Rui, Phys. Rev. C **28**, 42 (1983).
[3] H. J. Hauser, M. Walz, F. Weng, G. Staudt, and P. K. Rath, Nucl. Phys. **A456**, 253 (1986).
[4] A. Barbadoro, F. Pellegrini, G. F. Segato, L. Taffara, I. Gabrielli, and M. Bruno, Nucl. Phys. **C41**, 2425 (1990).
[5] G. S. Mani, D. Jacques, and A. D. B. Dix, Nucl. Phys. **A165**, 145 (1971).
[6] P. D. Kunz, University of Colorado report (unpublished).
[7] R. M Devries, J.-L. Perrenoud, I. Slaus, and J. W. Sunier, Nucl. Phys. **A178**, 424 (1972).
[8] S. Cohen and D. Kurath, Nucl. Phys. **73**, 1 (1965).
[9] D. Kurath and D. J. Millener, Nucl. Phys. **A238**, 269 (1975).
[10] D. Kurath, Phys. Rev. C **7**, 1390 (1973).
[11] A. G. M. van Hees and P. W. M. Glaudemans, Z. Phys. A **314**, 323 (1983); **315**, 223 (1984).
[12] A. A. Wolters, A. G. M. van Hees, and P. W. M. Glaudemans, Phys. Rev. C **42**, 2053 (1990); **42**, 2062 (1990).
[13] A. Nadasen, P. G. Roos, N. S. Chant, C. C. Chang, G. Ciangaru, H. F. Breuer, J. Wesick, and E. Norbeck, Phys. Rev. C **40**, 1130 (1989).